Bmp Signaling Governs Biliary-Driven Liver Regeneration in Zebrafish via Tbx2b and Id2a

Tae-Young Choi[1,5,7], **Mehwish Khaliq**[1,7], **Shinya Tsurusaki**[2], **Nikolay Ninov**[3,4,6], **Didier Y.R. Stainier**[3,4], **Minoru Tanaka**[2], and **Donghun Shin**[1,*]

[1]Department of Developmental Biology, Pittsburgh Liver Research Center, McGowan Institute for Regenerative Medicine, University of Pittsburgh, Pittsburgh, PA 15260, USA

[2]Department of Regenerative Medicine, Research Institute, National Center for Global Health and Medicine, Tokyo, Japan

[3]Department of Biochemistry and Biophysics, Programs in Developmental and Stem Cell Biology, Genetics and Human Genetics, Diabetes Center, and Liver Center, University of California, San Francisco, San Francisco, CA 94158, USA

[4]Department of Developmental Genetics, Max Planck Institute for Heart and Lung Research, 61231 Bad Nauheim, Germany

Abstract

Upon mild liver injury, new hepatocytes originate from pre-existing hepatocytes. However, if hepatocyte proliferation is impaired, a manifestation of severe liver injury, biliary epithelial cells (BECs) contribute to new hepatocytes through BEC dedifferentiation into liver progenitor cells (LPCs), also termed oval cells or hepatoblast-like cells (HB-LCs), and subsequent differentiation into hepatocytes. Despite the identification of several factors regulating BEC dedifferentiation and activation, little is known about factors involved in the regulation of LPC differentiation into hepatocytes during liver regeneration. Using a zebrafish model of near-complete hepatocyte ablation, we here show that Bmp signaling is required for BEC conversion to hepatocytes, particularly for LPC differentiation into hepatocytes. We found that severe liver injury led to the upregulation of genes involved in Bmp signaling, including *smad5*, *tbx2b*, and *id2a*, in the liver. Bmp suppression did not block BEC dedifferentiation into HB-LCs; however, the differentiation of HB-LCs into hepatocytes was impaired due to the maintenance of HB-LCs in an undifferentiated state. Later Bmp suppression did not affect HB-LC differentiation, but increased BEC number through proliferation. Notably, *smad5*, *tbx2b*, and *id2a* mutants exhibited similar liver regeneration defects as those observed in Bmp-suppressed livers. Moreover, BMP2 addition promoted the differentiation of a murine LPC cell line into hepatocytes *in vitro. Conclusions:* Bmp signaling regulates BEC-driven liver regeneration via *smad5*, *tbx2b* and *id2a*: it regulates HB-LC

*Correspondence: Donghun Shin, 3501 5th Ave. #5063 Pittsburgh, PA 15260, 1-412-624-2144 (phone), 1-412-383-2211 (fax), donghuns@pitt.edu.
[5]Current address: Department of Genetic Resources Research, National Marine Biodiversity Institute of Korea, Seocheon-gun, Chungcheongnam-do 33662, Korea
[6]Current address: DFG Research Center for Regenerative Therapies Dresden, Technische Universitat Dresden, Dresden, Germany
[7]These authors contribute equally to this work.

differentiation into hepatocytes via *tbx2b* and BEC proliferation via *id2a*. Our findings provide insights into promoting innate liver regeneration as a novel therapy.

Keywords

liver progenitor cells; oval cells; biliary epithelial cells; dedifferentiation; *smad5*

Introduction

As a highly regenerative organ, the liver can undergo either hepatocyte- or biliary-driven regeneration. In the former case, upon partial hepatectomy or mild liver injury, hepatocytes proliferate to restore the lost liver mass (1). However, in the latter case, upon severe liver injury in which hepatocyte proliferation is compromised, biliary epithelial cells (BECs) dedifferentiate into liver progenitor cells (LPCs), also called oval cells or hepatoblast-like cells (HB-LCs), and subsequently give rise to hepatocytes (2). Previously, controversies existed regarding the relative contribution of BEC-driven liver regeneration (3); however, recent studies in zebrafish (4, 5) and mice (6) have resolved this controversy by showing the extensive contribution of BECs to hepatocytes upon severe liver injury. In mice, hepatocyte-specific *Mdm2* deletion completely blocks hepatocyte proliferation, additionally induces hepatocyte senescence and apoptosis, and subsequently elicits oval cell activation. These oval cells later give rise to hepatocytes, leading to a full liver recovery (6). In the zebrafish studies, the near-complete ablation of hepatocytes elicits the extensive contribution of BECs to hepatocytes through the dedifferentiation of BECs into HB-LCs and subsequent differentiation of the HB-LCs into hepatocytes (4, 5)

Oval cells are frequently observed in diseased livers and their number positively correlates with disease severity (7). Since patients suffering from severe liver diseases have limited treatment options and present with an abundance of hepatic oval cells, promoting the differentiation of oval cells into hepatocytes is deemed an effective therapeutic strategy. Developing such therapies requires a deeper understanding of the mechanisms by which oval cells differentiate into hepatocytes *in vivo*. Although several factors, such as FGF7 (8) and TWEAK (9), which can induce oval cell activation *in vivo*, have been identified, factors that regulate oval cell differentiation into hepatocytes *in vivo* are unknown, mainly due to the lack of an animal model for BEC-driven liver regeneration. However, the recent reports of zebrafish and mouse liver injury models, in which BECs extensively contribute to regenerated hepatocytes, present an opportunity to investigate the mechanisms underlying oval cell differentiation into hepatocytes.

Using the zebrafish BEC-driven liver regeneration model combined with targeted chemical screening, we recently reported on the role of bromodomain extraterminal (BET) proteins in BEC dedifferentiation into HB-LCs and the proliferation of newly-generated hepatocytes (10). Using the same zebrafish model, we now show the essential role of Bmp signaling in HB-LC differentiation into hepatocytes. Bmp signaling plays important roles in early liver development, such as hepatoblast specification and proliferation (11, 12). Despite its clear role in early liver development, the role of Bmp signaling in liver regeneration has not been

clearly defined. Current literature provides confounding results that BMP2 (13) and BMP4 (14) negatively while BMP7 (15) positively regulate hepatocyte-driven liver regeneration after partial hepatectomy in rodents. Moreover, there is no report on the role of Bmp signaling in BEC-driven liver regeneration. Given the important role of Bmp signaling in early liver development and its positive effect on regeneration of other organs, including the heart (16), we hypothesized that Bmp signaling might regulate BEC-driven liver regeneration. Our finding that the hepatic expression of several genes implicated in Bmp signaling, including *smad5*, was upregulated during BEC-driven liver regeneration further supported our hypothesis. In this study, we report that Bmp signaling regulates two distinct steps of BEC-driven liver regeneration: (1) HB-LC differentiation into hepatocytes, and (2) the proliferation of newly-generated BECs.

Experimental procedures

Zebrafish lines

Experiments were performed with approval of the Institutional Animal Care and Use Committee at the University of Pittsburgh. We used *smad5*^{m169}, *tbx2b*^{c144}, and *id2a*^{pt661} mutant and the following transgenic lines: *Tg(fabp10a:rasGFP)*^{s942}, *Tg(Tp1:VenusPEST)*^{s940}, *Tg(Tp1:H2B-mCherry)*^{s939}, *Tg(ubb:loxP-EGFP-loxP-mCherry)*^{cz1701}, *Tg(Tp1:CreERT2)*^{s959}, *Tg(fabp10a:CFP-NTR)*^{s931}, *Tg(hs:dnBmpr1)*^{w30}, *Tg(fabp10a:CreERT2)*^{pt602}, *Tg(WRE:d2GFP)*^{kyu1}, and *Tg(Tp1:mAGFP-gmnn)*^{s707}. Their full names and references are listed in Table S1.

Hepatocyte ablation and DMH1 treatment

Hepatocyte ablation was performed by treating *Tg(fabp10a:CFP-NTR)* larvae with 10 mM Mtz in egg water supplemented with 0.2% DMSO and 0.2 mM 1-phenyl-2-thiourea, as previously described (17). To suppress Bmp signaling, 10 μM DMH1 (Tocris, Bristol, UK) was used.

RNAseq analysis

Over 100 livers were manually dissected for each condition (three non-ablating controls at 4.25, 5.25, and 6 days post-fertilization (dpf) and four regenerating livers at A18h, R6h, R12h, and R24h); total RNA was extracted from the dissected livers using the RNeasy Mini Kit (Qiagen, Valencia, CA). This RNA preparation was repeated three times and three-replicate RNA samples were mixed. These mixed samples were processed for single-end deep-transcriptome sequencing using the Illumina HiSeq 2000 platform, of which service was provided from Tufts University Core Facility. Galaxy was used to analyze the sequencing reads.

Additional methods are available in Supporting Information.

Results

Bmp signaling is required for BEC-driven liver regeneration

We have established a zebrafish liver injury model in which BECs extensively contribute to hepatocytes (4). Specifically, *Tg(fabp10a:CFP-NTR)* fish express nitroreductase (NTR) under the hepatocyte-specific *fabp10a* promoter; the treatment of metronidazole (Mtz), which is converted into a cytotoxic drug by NTR, results in hepatocyte-specific ablation in the transgenic fish. In this model, severe hepatocyte ablation induces the dedifferentiation of BECs into HB-LCs, which then differentiate into hepatocytes, thereby leading to a full liver recovery. To understand the molecular mechanisms underlying BEC-driven liver regeneration, we performed RNAseq analyses and compared gene expression profiles between control and regenerating livers at multiple time points during the regeneration. Through this analysis and subsequent validation with RT-PCR and whole-mount in situ hybridization (WISH) (Fig. S1), we found that genes implicated in the Bmp signaling pathway, such as *smad5*, *id2a*, and *tbx2b*, were upregulated in regenerating livers at regeneration (R) 6h compared with controls (Fig. 1A–1C). Bmp signaling plays an essential role in hepatoblast specification and liver growth during liver development (11, 12), but its role in liver regeneration has not been clearly defined. Thus, to determine whether Bmp signaling was required for BEC-driven liver regeneration, we applied the selective Bmp inhibitor, DMH1, which has been widely used in zebrafish. During BEC-driven liver regeneration, a hepatoblast/hepatocyte marker, Hnf4a, is induced in BECs and the expression of Prox1, a marker for hepatoblasts, hepatocytes, and BECs, is also upregulated in BECs (4). In addition, the expression of Alcam, a good marker of zebrafish BECs (18), is sustained in HB-LCs, but disappears from HB-LCs when these cells differentiate into hepatocytes (4). DMH1 treatment from ablation (A) 0h greatly repressed Hnf4a, but not Prox1 or Alcam, expression, at R0h (Fig. 1D). Intriguingly, DMH1 treatment after hepatocyte ablation (from R0h) significantly increased the number of BECs at R30h, as assessed by Alcam and *Tp1*:H2B-mCherry expression (Fig. 1E). The *Tg(Tp1:H2B-mCherry)* line, which expresses stable H2B-mCherry fusion proteins under the *Tp1* promoter containing the Notch-responsive element, reveals BECs in the liver (19). Collectively, these data indicate the essential roles of Bmp signaling in BEC-driven liver regeneration.

Inhibition of Bmp signaling blocks HB-LC differentiation into hepatocytes

Next, we investigated in detail the effect of Bmp inhibition on earlier stages of BEC-driven liver regeneration. We first determined if Bmp inhibition blocked the dedifferentiation of BECs into HB-LCs. By examining Hnf4a expression at various time points between A24h and A36h, we found that Hnf4a induction in BECs occurred around A33h and that its expression became stronger at A36h (Fig. S2A, arrows). As Hnf4a induction in BECs is indicative of BEC dedifferentiation (4), these data suggest that BECs dedifferentiate into HB-LCs around A33h. This observation was further supported by the expression of *fabp10a*:rasGFP (Fig. S2B), which is not expressed in hepatoblasts during liver development but induced in BECs during BEC-driven liver regeneration (10). At A33h, there were *fabp10a*:rasGFP+ cells negative for Hnf4a (Fig. S2C, arrows), but not vice versa, indicating that *fabp10a* induction in BECs precedes Hnf4a induction. Although Hnf4a expression in

BEC-derived cells was greatly reduced at A36h in DMH1-treated regenerating livers compared with their controls (Fig. 1D), the initial induction of Hnf4a and *fabp10a*:rasGFP in BECs at A33h appeared unaffected in DMH1-treated regenerating livers (Fig. S2A and S2B). These data together with normal Prox1 expression in HB-LCs indicate that Bmp inhibition does not block the dedifferentiation of BECs.

Given that Hnf4a is the master regulator of hepatocyte differentiation (20), the reduced Hnf4a expression upon Bmp inhibition (Fig. 1D) suggests a role for Bmp signaling in HB-LC differentiation into hepatocytes. To address this possibility, we sought to examine DMH1-treated regenerating larvae at later stages, such as R24h. However, the continuous DMH1 treatment from A0h killed most regenerating larvae before R24h, preventing the examination of the regenerating livers at later stages. By treating ablating larvae with DMH1 from different time points, we found that DMH1 treatment from A33h also reduced Hnf4a expression at R6h (Fig. 2A) but did not kill regenerating larvae as late as R24h. At R24h, A33h DMH1-treated regenerating livers exhibited the following phenotypes: (1) sustained Alcam expression in most BEC-derived *Tp1*:H2B-mCherry$^+$ cells (Fig. 2B); (2) sustained Notch activity, as revealed by *Tp1*:VenusPEST expression (21), throughout regenerating livers, (Fig. 2C); and (3) no expression of hepatocyte markers, Bhmt, *cp*, and *gc* (Fig. 2D and 2E), indicating a defect in HB-LC differentiation into hepatocytes. Despite a lack of hepatocyte marker expression, the expression of *foxa3* and *prox1a*, which are expressed in hepatoblasts, was unaffected in DMH1-treated regenerating livers (Fig. 2E). *fabp10a*, which is expressed in HB-LCs (Fig. S2B), expression was also unaffected (Fig. 2D and 2E). In addition to the pharmacologic inhibition, we blocked Bmp signaling using the *Tg(hs:dnBmpr1)* line that expresses dominant-negative Bmpr1 under the *hsp70l* heat-shock promoter. The overexpression of dnBmpr1 via a single heat-shock at A30h resulted in sustained Notch activity and reduced Hnf4a expression in regenerating livers at R12h (Fig. 2F). All these data indicate the role of Bmp signaling in HB-LC differentiation into hepatocytes.

Inhibition of Bmp signaling maintains HB-LCs in their undifferentiated state

Based on sustained Notch activity and Alcam expression in A33h DMH1-treated regenerating livers, we hypothesized that HB-LCs that failed to differentiate into hepatocytes remained as undifferentiated HB-LCs in DMH1-treated regenerating livers. To test this hypothesis, we used Cre/loxP-mediated lineage tracing and determined the lineages of HB-LCs. To label HB-LCs, we used two Cre lines, *Tg(Tp1:CreERT2)* that expresses CreERT2 under the *Tp1* promoter (22) and *Tg(fabp10a:CreERT2)* that expresses CreERT2 under the *fabp10a* promoter (4). Since Notch activity is strong in BECs but weak in HB-LCs, the former line labels most BECs but a few HB-LCs. Likewise, since *fabp10a* expression is strong in hepatocytes but weak in HB-LCs, the latter line labels most hepatocytes but a few HB-LCs. When *Tp1*:CreERT2 and *fabp10a*:CreERT2 were activated by tamoxifen (4-OHT) treatment from A33h to R6h, 95% of BECs and 96% of hepatocytes, respectively, were labeled at R54h (Fig. 3B). However, few hepatocytes were labeled by the *Tp1*:CreERT2 activation (Fig. 3C) and few BECs were labeled by the *fabp10a*:CreERT2 activation (Fig. 3D), indicating that few HB-LCs were labeled in these Cre activation settings. This low efficiency of HB-LC labeling can be explained by the weak Notch activity and weak

fabp10a expression in HB-LCs and the short duration of HB-LCs in the zebrafish liver injury model. If the HB-LCs fail to differentiate and remain in a progenitor-like state, more HB-LCs will be labeled in the Cre activation settings, thereby more hepatocytes and BECs were labeled by *Tp1*:CreERT2 and *fabp10a*:CreERT2, respectively. We observed these phenomena in regenerating livers treated with DMH1 from A33h to R6h (Fig. 3C and 3D), strongly suggesting that Bmp inhibition maintains HB-LCs in their undifferentiated state.

Inhibition of Bmp signaling after hepatocyte ablation increases BEC number in regenerating livers via proliferation

Unlike its treatment from A33h, DMH1 treatment from R0h did not affect HB-LC differentiation into hepatocytes, as assessed by *cp* and *gc* expression (Fig. S3). Given the increased number of BECs upon DMH1 treatment from R0h (Fig. 1E), we determined the latest time point from which DMH1 treatment still increased BEC number. We found that DMH1 treatment from R12h, but not R24h, significantly increased BEC number (Fig. 4A). Using a cell-cycle reporter line, *Tg(Tp1:mAGFP-gmnn)*, which reveals BECs in the S/G2/M (but not G0/G1) phases of the cell cycle, we observed that BEC proliferation was significantly increased in DMH1-treated regenerating livers at R30h compared with their controls (Fig. 4B). In addition to the chemical inhibition of Bmp signaling, the overexpression of dnBmpr1 via a single heat-shock at R8h increased BEC proliferation in regenerating livers at R30h (Fig. 4C and 4D). Altogether, these data indicate that Bmp signaling controls the number of BECs in regenerating livers by temporarily suppressing their proliferation.

smad5 mutants exhibit a defect in HB-LC differentiation into hepatocytes

Given the upregulation of genes implicated in Bmp signaling, such as *smad5, tbx2b*, and *id2a*, in regenerating livers (Fig. 1A–1C), we determined if DMH1 treatment suppressed this upregulation. Indeed, quantitative RT-PCR (qPCR) and WISH showed a reduction of the hepatic expression of *smad5, tbx2b*, and *id2a* in DMH1-treated regenerating livers at R6h compared with their controls (Fig. 5A), suggesting a potential role for these genes in mediating Bmp signaling during BEC-driven liver regeneration. To test this possibility, we examined BEC-driven liver regeneration in *smad5* mutants. Smad5, together with Smad1 and Smad9, known as receptor-regulated Smads (R-Smads), relays Bmp signaling from the cell surface to the nucleus (23). Zebrafish *smad5*$^{-/-}$ mutants started to die from 3 dpf but *smad5* mRNA injection into one-cell-stage embryos increased their survival time (24), allowing for our liver regeneration assay. Although the mRNA-injected mutants had a smaller liver than their siblings, liver development occurred, as observed by their liver growth (Fig. S4B) and the branching of the intrahepatic biliary structure (Fig. S4C). Since liver size was smaller in the mRNA-injected mutants than in wild-type, we applied Mtz from 5 dpf, when the mutant liver size is similar to that of 3.5-dpf wild-type liver. In this rescue setting, the *smad5*$^{-/-}$ mutants exhibited sustained Notch activity and Alcam expression throughout regenerating livers (Fig. 5B–5D) and no *cp*, but faint *gc*, expression (Fig. 5E) at R24h, recapitulating the HB-LC differentiation defects observed in A33h DMH1-treated regenerating livers. The expression of *tbx2b* and *id2a* in regenerating livers also appeared to be reduced in the *smad5*$^{-/-}$ mutants compared with their siblings (Fig. 5E), further supporting that Bmp signaling regulates *tbx2b* and *id2a* expression in regenerating livers.

When examined at R48h, continuous DMH1 treatment from A33h was fatal for the zebrafish larvae recovering from severe liver injury, preventing the analysis of BEC-driven liver regeneration at later stages. However, the $smad5^{-/-}$ mutants recovered at R48h from the initial regeneration defects, as displayed by the rapid growth of their regenerating livers (Fig. S4E), normal Notch activity (Fig. S4F), and recovered cp and gc expression (Fig. S4G). Altogether, data from $smad5$ mutant analyses indicate the role of $smad5$ in BEC-driven liver regeneration.

tbx2b mutants exhibit a defect in HB-LC differentiation into hepatocytes

TBX3, a T-box transcription factor, promotes hepatoblast proliferation and maintains the expression of HNF4A and CEBPA, two key transcription factors regulating hepatocyte differentiation, in hepatoblasts (25). TBX2, a close homolog of TBX3, is required for the development of the heart, pharyngeal arch, and optic cup; importantly, its expression in these tissues is regulated by Bmp signaling (26). Thus, to determine if $tbx2b$ was required for BEC-driven liver regeneration, we used zebrafish $tbx2b$ mutants because they develop with normal body morphology (Fig. S5A) and survive long enough for our liver regeneration assay (27). Despite the absence of liver developmental defects (Fig. S5B), $tbx2b^{-/-}$ mutants exhibited a defect in HB-LC differentiation into hepatocytes during BEC-driven liver regeneration. In control regenerating livers, all $Tp1$:VenusPEST$^-$/$Tp1$:H2B-mCherry$^+$ cells expressed Hnf4a and Bhmt at R24h, indicating that they are hepatocytes derived from BECs. However, in $tbx2b^{-/-}$ regenerating livers, many $Tp1$:VenusPEST$^-$/Tp1:H2B-mCherry$^+$ cells not only failed to express Hnf4a and Bhmt (Fig. 6A–6C), but also showed sustained Alcam expression at R24h (Fig. 6D). This phenotype was severe in ~40% of the mutants, having few Bhmt$^+$ hepatocytes, but mild in the rest of them, having a significant number of the hepatocytes (Fig. 6B–6D). To determine whether the observed phenotype at R24h later recovered, we examined regenerating livers at R48h. All mutants at R48h still contained a significant number of $Tp1$:VenusPEST$^-$/Tp1:H2B-mCherry$^+$ cells negative for Hnf4a (Fig. S5C), suggesting that in the absence of Tbx2b, BEC-derived cells that failed to differentiate into hepatocytes at R24h do not recover at a later time point. We next examined if BEC dedifferentiation was affected in $tbx2b^{-/-}$ mutants. Although Hnf4a expression in regenerating livers at R6h was reduced in the mutants compared with their siblings, $fabp10a$:rasGFP expression appeared unaffected in the mutants (Fig. S5D), suggesting that BECs dedifferentiate into HB-LCs in the absence of Tbx2b. Altogether, data from $tbx2b$ mutant analyses indicate the crucial role of $tbx2b$ in BEC-driven liver regeneration, in particular, HB-LC differentiation into hepatocytes.

id2a mutants temporarily display an excess of BECs in regenerating livers

$Id2$ is a well-known downstream target gene of Bmp signaling in many tissues, including pancreatic epithelia (28); the mouse $Id2$ promoter contains BMP-responsive elements (29). $id2a$, the zebrafish orthologue of mouse $Id2$, is also regulated by Bmp signaling in cranial neural crest cells (30). Not only are $Id2$ and $id2a$ the direct targets of Bmp signaling, but they also mediate the effect of Bmp signaling in these tissues. Given its BEC-specific expression in the developing liver (31) and its regulation by Bmp signaling in regenerating livers (Fig. 5A), we hypothesized that $id2a$ served as a mediator of Bmp signaling in BEC-driven liver regeneration. Using transcription activator-like effector nuclease (TALEN) genome editing

technology, we generated *id2a* mutants containing a 22-bp deletion in its first exon. The mutant larvae did not exhibit any liver developmental defects (Fig. S6A and S6B) and grew normally to adults. BEC-driven liver regeneration appeared unaffected in *id2a*$^{-/-}$ mutants, as assessed by Hnf4a expression at R6h (Fig. 7B) and *gc* expression at R24h (Fig. 7C); however, the mutant regenerating livers had significantly more BECs than controls at R30h (Fig. 7D), resembling the excessive BEC phenotype seen in regenerating livers treated with DMH1 from R0h. This increased BEC number was due to increased proliferation, as revealed by EdU labeling (Fig. 7E). However, this BEC phenotype was temporary because there was no difference in BEC number between wild-type and *id2a*$^{-/-}$ mutant regenerating livers at R72h (Fig. S6C). Altogether, data from *id2a* mutant analyses suggest that *id2a* mediates, in part, the effect of Bmp signaling on BEC proliferation during BEC-driven liver regeneration.

BMP2 addition promotes the differentiation of a murine liver progenitor cell line into hepatocytes *in vitro*

To explore whether the findings from the zebrafish liver injury model can be translated to mammals, we used a murine liver progenitor cell line that was established from DDC diet-fed mice (32). These cells can efficiently differentiate into hepatocytes or BECs depending on culture conditions (32). In the hepatocyte differentiation condition, addition of BMP2 significantly increased the expression of three hepatocyte markers, *G6pc*, *Tat*, and *Tdo2* (Fig. 8), consistent with the findings in zebrafish.

Discussion

Using the zebrafish hepatocyte ablation model, we elucidate two distinct roles of Bmp signaling in BEC-driven liver regeneration: (1) initially, Bmp signaling regulates HB-LC differentiation into hepatocytes; (2) later, Bmp signaling controls the proliferation of newly-generated BECs. By analyzing the mutants of *smad5*, *tbx2b*, and *id2a*, genes involved in the Bmp signaling pathway, we discovered that Smad5 is the main receptor-regulated Smad during BEC-driven liver regeneration and that Tbx2b and Id2a mediate its effect on HB-LC differentiation into hepatocytes and on BEC proliferation, respectively.

Bmp (11, 12), Fgf (12, 33), and Wnt/β-catenin signaling (34) are implicated in hepatoblast specification and proliferation during liver development. Given that regeneration often recapitulates development and key developmental factors are re-utilized during regeneration, these signaling pathways may also regulate liver regeneration. During hepatocyte-driven liver regeneration, both Wnt/β-catenin (35) and Fgf signaling (36) promote hepatocyte proliferation. During BEC-driven liver regeneration, Wnt/β-catenin signaling promotes oval cell proliferation (37) and Fgf signaling induces oval cell activation (8). In contrast to Wnt/β-catenin and Fgf signaling, the influence of Bmp signaling on hepatocyte proliferation during hepatocyte-driven liver regeneration is ligand-dependent: BMP4 signaling through Alk3 represses hepatocyte proliferation, whereas BMP7 signaling through Alk2 promotes hepatocyte proliferation (14). Previous *in vitro* studies have reported on the role of BMP signaling in the differentiation of LPCs into hepatocytes: BMP4 treatment induced the differentiation of rat hepatic progenitor cells (38) and CD133^{+} hepatic cancer stem cells (39)

into hepatocytes. Our *in vitro* and *in vivo* data support these findings and further reveal the crucial role of Bmp signaling in BEC-driven liver regeneration, specifically during the differentiation phase of LPCs into hepatocytes.

To further elucidate the mechanisms by which Bmp signaling controls BEC-driven liver regeneration, we analyzed *tbx2b* and *id2a* mutants. Our RNAseq data revealed that at R6h, both *tbx2b* (among the T-box transcription factor genes) and *id2a* (among the Id family genes) were highly upregulated in regenerating livers compared with the other *tbx* and *id* genes (Fig. S7A and S7B), suggesting their importance in BEC-driven liver regeneration. As expected, both *tbx2b* and *id2a* expression decreased in both DMH1-treated and *smad5*$^{-/-}$ regenerating livers. Importantly, *tbx2b*$^{-/-}$ mutants exhibited a defect in HB-LC differentiation into hepatocytes and *id2a* mutants exhibited excessive BECs in regenerating livers at R30h, revealing *tbx2b* and *id2a* as the key downstream mediators of Bmp signaling that regulates BEC-driven liver regeneration.

Using a morpholino-mediated knockdown approach, we previously reported that during liver development, Id2a positively regulates hepatic outgrowth through hepatoblast proliferation and survival (31). However, we found that during BEC-driven liver regeneration, Id2a negatively regulates the proliferation of newly-generated BECs. Although we did not detect any developmental defects in the *id2a*$^{-/-}$ mutants, inconsistent with the morpholino results, this discrepancy might be explained by the genetic compensations that can occur in mutants but not in morphants (40). Previous rodent studies have highlighted the role of *Id1* and *Id2* in hepatocyte-driven liver regeneration. Following partial hepatectomy, not only *Id1* was upregulated in liver sinusoidal endothelial cells (LSECs), but *Id1*$^{-/-}$ mice displayed abnormal liver function and impaired liver regeneration (41). In fact, following acute liver injury, *Id1* was induced downstream of LSEC-specific upregulation of CXCR4/CXCR7 (42). As a result, ID1 promotes the secretion of pro-regenerative angiocrine factors, such as Wnt2 and HGF, to aid in hepatocyte proliferation after liver injury (41, 42). Similar to *Id1*, *Id2* levels also increased after partial hepatectomy and bile duct ligation in rats (43), but its role in liver regeneration has not yet been reported.

While Wnt/β-catenin signaling promotes LPC differentiation into hepatocytes, Notch signaling represses the process (44, 45). Here, we presented Bmp signaling as another regulator of this differentiation process. Since we did not observe any changes in Wnt activity between DMSO- and DMH1-treated regenerating livers (Fig. S8), it appears that Bmp signaling does not affect Wnt/β-catenin signaling. However, sustained, weak Notch activity observed in DMH1-treated regenerating livers suggests that Bmp signaling may suppress Notch signaling. Although it was reported that repression of Notch signaling promotes LPC differentiation into hepatocytes (44, 45), the hepatocyte differentiation defects observed in DMH1-treated livers were not rescued by inhibiting Notch signaling globally (data not shown). Thus, it is unlikely that Bmp signaling controls LPC differentiation through Wnt/β-catenin or Notch signaling. However, we do not exclude the possibility that Wnt/β-catenin and Notch signaling control LPC differentiation through Bmp signaling.

The zebrafish hepatocyte ablation model has contributed significantly to a better understanding of BEC- or LPC-driven liver regeneration. We previously reported that Wnt/ β-catenin signaling via Wnt2bb regulates the proliferation of newly-generated hepatocytes (4) and that BET proteins regulate BEC dedifferentiation and the proliferation and maturation of newly-generated hepatocytes (10). Using the same model, others also reported on the involvement of Notch signaling in BEC-driven liver regeneration (46). Here, we provide the gene expression profiles of regenerating livers at four distinct stages, A18h, R6h, R12h, and R24h. Although we focus on Bmp signaling and its downstream target genes in this study, these expression profiles will be useful for identifying other crucial genes involved in regulating BEC-driven liver regeneration.

In summary, we discovered that Bmp signaling regulates HB-LC differentiation into hepatocytes, partly, via Tbx2b and controls the proliferation of newly-generated BECs via Id2a. Liver biopsies of human patients suffering from chronic liver diseases display an abundance of oval cells, also known as HB-LCs. To promote the differentiation of these oval cells into hepatocytes in these patients, one possible therapy may involve enhancing hepatic Bmp signaling.

Supplementary Material

Refer to Web version on PubMed Central for supplementary material.

Acknowledgments

List of abbreviations

BEC	biliary epithelial cell
LPCs	liver progenitor cells
HB-LCs	hepatoblast-like cells
BET	bromodomain extraterminal
Mtz	metronidazole
dpf	days post-fertilization
NTR	nitroreductase
WISH	whole-mount in situ hybridization
4-OHT	tamoxifen

|	
qPCR	quantitative RT-PCR
TALEN	transcription activator-like effector nuclease
LSECs	liver sinusoidal endothelial cells

References

Author names in bold designate shared co-first authorship.

1. Michalopoulos GK. Liver regeneration. J Cell Physiol. 2007; 213:286–300. [PubMed: 17559071]

2. Miyajima A, Tanaka M, Itoh T. Stem/Progenitor Cells in Liver Development, Homeostasis, Regeneration, and Reprogramming. Cell Stem Cell. 2014; 14:561–574. [PubMed: 24792114]

3. Greenbaum LE. The Ductal Plate: A Source of Progenitors and Hepatocytes in the Adult Liver. Gastroenterology. 2011; 141:1152–1155. [PubMed: 21875588]

4. Choi TY, Ninov N, Stainier DY, Shin D. Extensive conversion of hepatic biliary epithelial cells to hepatocytes after near total loss of hepatocytes in zebrafish. Gastroenterology. 2014; 146:776–788. [PubMed: 24148620]

5. He J, Lu H, Zou Q, Luo L. Regeneration of liver after extreme hepatocyte loss occurs mainly via biliary transdifferentiation in zebrafish. Gastroenterology. 2014; 146:789–800. e788. [PubMed: 24315993]

6. Lu W-Y, Bird TG, Boulter L, Tsuchiya A, Cole AM, Hay T, Guest RV, et al. Hepatic progenitor cells of biliary origin with liver repopulation capacity. Nature Cell Biology. 2015; 17:971–983. [PubMed: 26192438]

7. Lowes KN, Brennan BA, Yeoh GC, Olynyk JK. Oval cell numbers in human chronic liver diseases are directly related to disease severity. American Journal of Pathology. 1999; 154:537–541. [PubMed: 10027411]

8. Takase HM, Itoh T, Ino S, Wang T, Koji T, Akira S, Takikawa Y, et al. FGF7 is a functional niche signal required for stimulation of adult liver progenitor cells that support liver regeneration. Genes Dev. 2013; 27:169–181. [PubMed: 23322300]

9. Bird TGT, Lu WW-Y, Boulter L, Gordon-Keylock S, Ridgway Ra, Williams MJ, Taube J, et al. Bone marrow injection stimulates hepatic ductular reactions in the absence of injury via macrophage-mediated TWEAK signaling. Proc Natl Acad Sci U S A. 2013; 110:6542–6547. [PubMed: 23576749]

10. Ko S, Choi TY, Russell JO, So J, Monga SPS, Shin D. Bromodomain and extraterminal (BET) proteins regulate biliary-driven liver regeneration. J Hepatol. 2016; 64:316–325. [PubMed: 26505118]

11. Rossi JM, Dunn NR, Hogan BL, Zaret KS. Distinct mesodermal signals, including BMPs from the septum transversum mesenchyme, are required in combination for hepatogenesis from the endoderm. Genes Dev. 2001; 15:1998–2009. [PubMed: 11485993]

12. Shin D, Shin CH, Tucker J, Ober EA, Rentzsch F, Poss KD, Hammerschmidt M, et al. Bmp and Fgf signaling are essential for liver specification in zebrafish. Development. 2007; 134:2041–2050. [PubMed: 17507405]

13. Xu CP, Ji WM, van den Brink GR, Peppelenbosch MP. Bone morphogenetic protein-2 is a negative regulator of hepatocyte proliferation downregulated in the regenerating liver. World Journal of Gastroenterology. 2006; 12:7621–7625. [PubMed: 17171790]

14. Do N, Zhao R, Ray K, Ho K, Dib M, Ren X, Kuzontkoski P, et al. BMP4 is a novel paracrine inhibitor of liver regeneration. Am J Physiol Gastrointest Liver Physiol. 2012; 303:G1220–1227. [PubMed: 23019195]

15. Sugimoto H, Yang CQ, LeBleu VS, Soubasakos MA, Giraldo M, Zeisberg M, Kalluri R. BMP-7 functions as a novel hormone to facilitate liver regeneration. Faseb Journal. 2007; 21:256–264. [PubMed: 17116741]

16. Wu CC, Kruse F, Vasudevarao MD, Junker JP, Zebrowski DC, Fischer K, Noel ES, et al. Spatially Resolved Genome-wide Transcriptional Profiling Identifies BMP Signaling as Essential Regulator of Zebrafish Cardiomyocyte Regeneration. Dev Cell. 2016; 36:36–49. [PubMed: 26748692]

17. Choi TY, Khaliq M, Ko S, So J, Shin D. Hepatocyte-specific ablation in zebrafish to study biliary-driven liver regeneration. J Vis Exp. 2015:e52785. [PubMed: 26065829]

18. Sakaguchi TF, Sadler KC, Crosnier C, Stainier DY. Endothelial signals modulate hepatocyte apicobasal polarization in zebrafish. Curr Biol. 2008; 18:1565–1571. [PubMed: 18951027]

19. Delous M, Yin C, Shin D, Ninov N, Debrito Carten J, Pan L, Ma TP, et al. Sox9b is a key regulator of pancreaticobiliary ductal system development. PLoS Genet. 2012; 8:e1002754. [PubMed: 22719264]

20. Si-Tayeb K, Lemaigre FP, Duncan SA. Organogenesis and development of the liver. Dev Cell. 2010; 18:175–189. [PubMed: 20159590]

21. Ninov N, Borius M, Stainier DYR. Different levels of Notch signaling regulate quiescence, renewal and differentiation in pancreatic endocrine progenitors. Development. 2012; 139:1557–1567. [PubMed: 22492351]

22. Ninov N, Hesselson D, Gut P, Zhou A, Fidelin K, Stainier DYR. Metabolic Regulation of Cellular Plasticity in the Pancreas. Current Biology. 2013; 23:1242–1250. [PubMed: 23791726]

23. Massague J, Wotton D. Transcriptional control by the TGF-beta/Smad signaling system. EMBO J. 2000; 19:1745–1754. [PubMed: 10775259]

24. Kramer C, Mayr T, Nowak M, Schumacher J, Runke G, Bauer H, Wagner DS, et al. Maternally supplied Smad5 is required for ventral specification in zebrafish embryos prior to zygotic Bmp signaling. Dev Biol. 2002; 250:263–279. [PubMed: 12376102]

25. Ludtke TH, Christoffels VM, Petry M, Kispert A. Tbx3 promotes liver bud expansion during mouse development by suppression of cholangiocyte differentiation. Hepatology. 2009; 49:969–978. [PubMed: 19140222]

26. Shirai M, Imanaka-Yoshida K, Schneider MD, Schwartz RJ, Morisaki T. T-box 2, a mediator of Bmp-Smad signaling, induced hyaluronan synthase 2 and Tgfbeta2 expression and endocardial cushion formation. Proc Natl Acad Sci U S A. 2009; 106:18604–18609. [PubMed: 19846762]

27. Snelson CD, Santhakumar K, Halpern ME, Gamse JT. Tbx2b is required for the development of the parapineal organ. Development. 2008; 135:1693–1702. [PubMed: 18385257]

28. Hua H, Zhang YQ, Dabernat S, Kritzik M, Dietz D, Sterling L, Sarvetnick N. BMP4 regulates pancreatic progenitor cell expansion through Id2. J Biol Chem. 2006; 281:13574–13580. [PubMed: 16547003]

29. Nakahiro T, Kurooka H, Mori K, Sano K, Yokota Y. Identification of BMP-responsive elements in the mouse Id2 gene. Biochem Biophys Res Commun. 2010; 399:416–421. [PubMed: 20674548]

30. Das A, Crump JG. Bmps and Id2a Act Upstream of Twist1 To Restrict Ectomesenchyme Potential of the Cranial Neural Crest. PLoS Genet. 2012:8.

31. Khaliq M, Choi TY, So J, Shin D. Id2a is required for hepatic outgrowth during liver development in zebrafish. Mech Dev. 2015; 138(Pt 3):399–414. [PubMed: 26022495]

32. Okabe M, Tsukahara Y, Tanaka M, Suzuki K, Saito S, Kamiya Y, Tsujimura T, et al. Potential hepatic stem cells reside in EpCAM(+) cells of normal and injured mouse liver. Development. 2009; 136:1951–1960. [PubMed: 19429791]

33. Jung J, Zheng M, Goldfarb M, Zaret KS. Initiation of mammalian liver development from endoderm by fibroblast growth factors. Science. 1999; 284:1998–2003. [PubMed: 10373120]

34. Ober EA, Verkade H, Field HA, Stainier DY. Mesodermal Wnt2b signalling positively regulates liver specification. Nature. 2006; 442:688–691. [PubMed: 16799568]

35. Nejak-Bowen KN, Thompson MD, Singh S, Bowen WC Jr, Dar MJ, Khillan J, Dai C, et al. Accelerated liver regeneration and hepatocarcinogenesis in mice overexpressing serine-45 mutant beta-catenin. Hepatology. 2010; 51:1603–1613. [PubMed: 20432254]

36. Padrissa-Altes S, Bachofner M, Bogorad RL, Pohlmeier L, Rossolini T, Bohm F, Liebisch G, et al. Control of hepatocyte proliferation and survival by Fgf receptors is essential for liver regeneration in mice. Gut. 2015; 64:1444–1453. [PubMed: 25416068]

37. Apte U, Thompson MD, Cui SS, Liu B, Cieply B, Monga SPS. Wnt/beta-catenin signaling mediates oval cell response in rodents. Hepatology. 2008; 47:288–295. [PubMed: 17929301]

38. Fan J, Shen H, Dai Q, Minuk GY, Burzynski FJ, Gong Y. Bone morphogenetic protein-4 induced rat hepatic progenitor cell (WB-F344 cell) differentiation toward hepatocyte lineage. J Cell Physiol. 2009; 220:72–81. [PubMed: 19229878]

39. Zhang L, Sun H, Zhao F, Lu P, Ge C, Li H, Hou H, et al. BMP4 administration induces differentiation of CD133+ hepatic cancer stem cells, blocking their contributions to hepatocellular carcinoma. Cancer Res. 2012; 72:4276–4285. [PubMed: 22773665]

40. Rossi A, Kontarakis Z, Gerri C, Nolte H, Holper S, Kruger M, Stainier DY. Genetic compensation induced by deleterious mutations but not gene knockdowns. Nature. 2015; 524:230–233. [PubMed: 26168398]

41. Ding BS, Nolan DJ, Butler JM, James D, Babazadeh AO, Rosenwaks Z, Mittal V, et al. Inductive angiocrine signals from sinusoidal endothelium are required for liver regeneration. Nature. 2010; 468:310–315. [PubMed: 21068842]

42. Ding BS, Cao Z, Lis R, Nolan DJ, Guo P, Simons M, Penfold ME, et al. Divergent angiocrine signals from vascular niche balance liver regeneration and fibrosis. Nature. 2014; 505:97–102. [PubMed: 24256728]

43. Rodriguez JL, Sandoval J, Serviddio G, Sastre J, Morante M, Perrelli MG, Martinez-Chantar ML, et al. Id2 leaves the chromatin of the E2F4-p130-controlled c-myc promoter during hepatocyte priming for liver regeneration. Biochem J. 2006; 398:431–437. [PubMed: 16776654]

44. Kitade M, Factor VM, Andersen JB, Tomokuni A, Kaji K, Akita H, Holczbauer A, et al. Specific fate decisions in adult hepatic progenitor cells driven by MET and EGFR signaling. Genes Dev. 2013; 27:1706–1717. [PubMed: 23913923]

45. Boulter L, Govaere O, Bird TG, Radulescu S, Ramachandran P, Pellicoro A, Ridgway RA, et al. Macrophage-derived Wnt opposes Notch signaling to specify hepatic progenitor cell fate in chronic liver disease. Nature Medicine. 2012; 18:572–579.

46. Huang MB, Chang A, Choi M, Zhou D, Anania FA, Shin CH. Antagonistic Interaction Between Wnt and Notch Activity Modulates the Regenerative Capacity of a Zebrafish Fibrotic Liver Model. Hepatology. 2014; 60:1753–1766. [PubMed: 24995814]
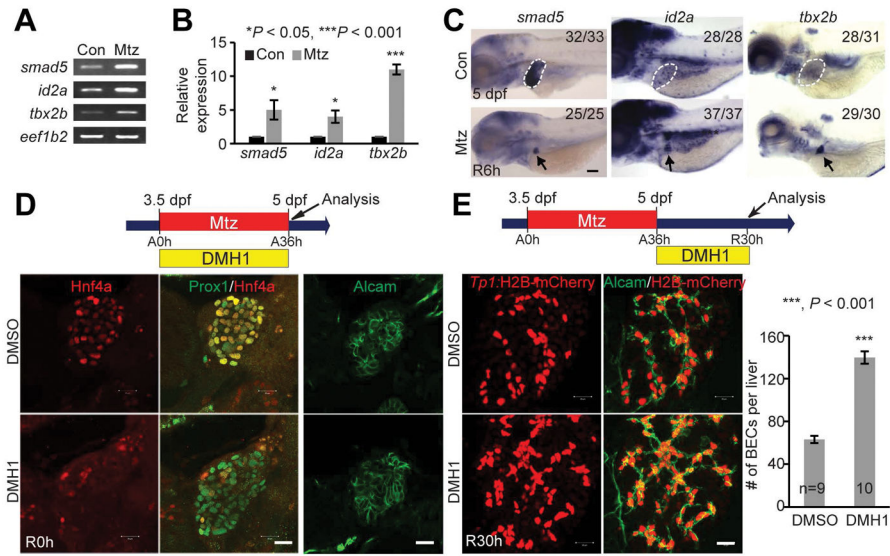
Figure 1. Bmp signaling is required for BEC-driven liver regeneration

(A, B) RT-PCR (A) and qPCR (B) data showing the expression levels of *smad5*, *id2a* and *tbx2b* between control and regenerating livers at R6h. (C) WISH images showing the expression of *smad5*, *id2a* and *tbx2b* in control (dashed lines) and regenerating (arrows) livers. Numbers indicate the proportion of larvae exhibiting the expression shown. (D) Single-optical section images showing the expression of Hnf4a and Prox1 or Alcam in regenerating livers. (E) Confocal projection images showing *Tp1*:H2B-mCherry and Alcam expression in regenerating livers. Quantification of the number of H2B-mCherry/Alcam double-positive cells (i.e., BECs). Scale bars: 150 (C), 20 (D,E) μm; error bars: ±SEM.
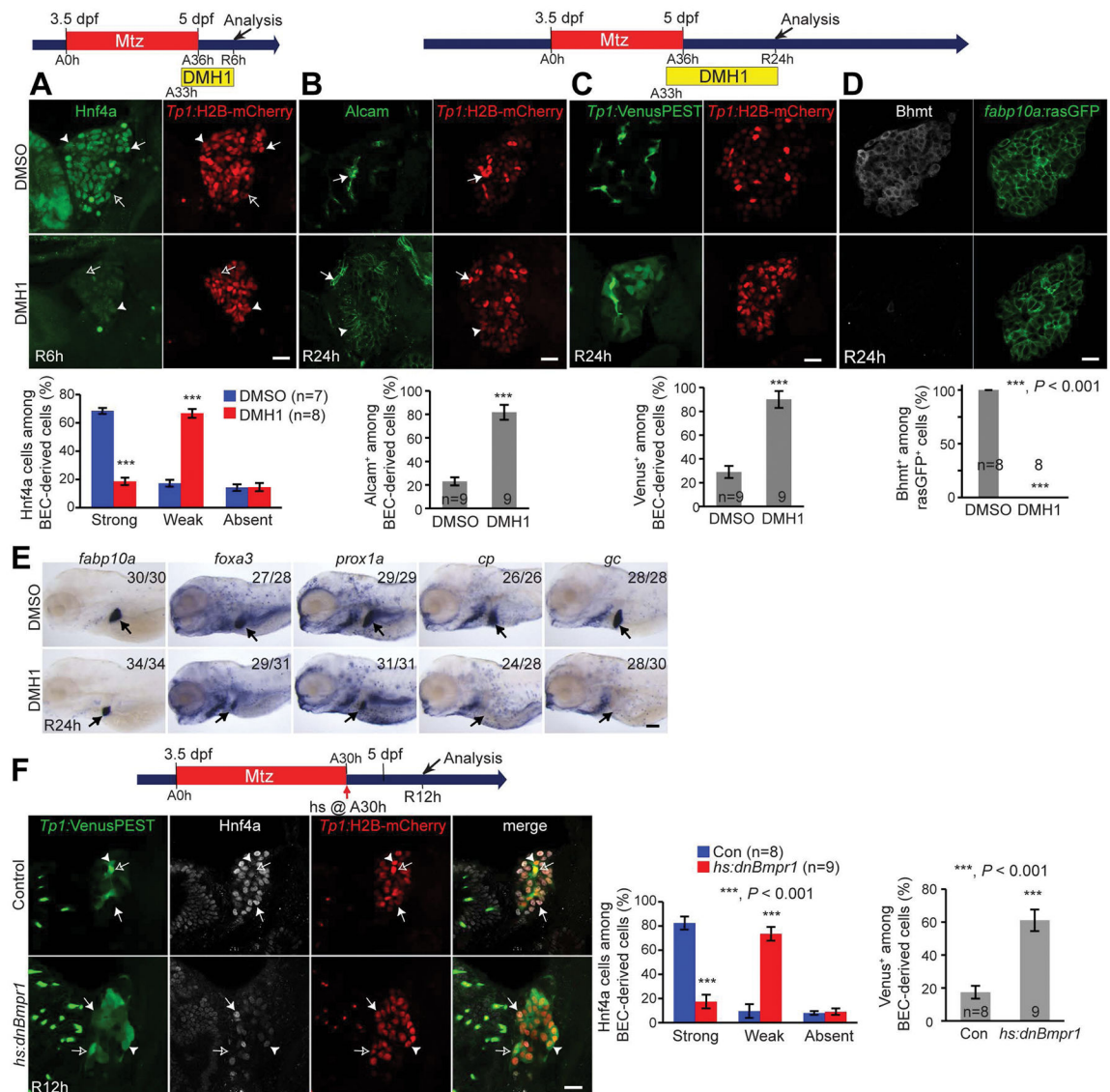
Figure 2. Bmp inhibition blocks HB-LC differentiation into hepatocytes

(A) Single-optical section images showing Hnf4a and *Tp1*:H2B-mCherry expression in regenerating livers. To quantify Hnf4a expression, BEC-derived H2B-mCherry$^+$ cells were divided into three cases: Hnf4a^{strong} (arrows), Hnf4a^{weak} (arrowheads), and Hnf4a^{absent} (open arrows). Quantification of the percentage of these three cell types among H2B-mCherry$^+$ cells. (B) Single-optical section images showing Alcam and *Tp1*:H2B-mCherry expression in regenerating livers. In DMH1-treated regenerating livers, Alcam was expressed in both H2B-mCherry^{strong} (arrows) and H2B-mCherry^{weak} cells (arrowheads), whereas in control regenerating livers, Alcam was expressed only in H2B-mCherry^{strong} cells. Quantification of the percentage of Alcam$^+$ cells among H2B-mCherry$^+$ cells. (C) Single-optical section images showing the expression of *Tp1*:VenusPEST and *Tp1*:H2B-mCherry in regenerating livers. Quantification of the percentage of VenusPEST$^+$ cells among H2B-mCherry$^+$ cells. (D) Single-optical section images showing Bhmt and *fabp10a*:rasGFP expression in regenerating livers. Quantification of the percentage of Bhmt$^+$

cells among BEC-derived *fabp10a*.rasGFP$^+$ cells. (E) WISH images showing the expression of *fabp10a*, *foxa3*, *prox1a*, *cp* and *gc* in regenerating livers (arrows). (F) Single-optical section images showing Hnf4a, *Tp1:*VenusPEST, and *Tp1:*H2B-mCherry expression in regenerating livers. The *Tg(hs:dnBmpr1-GFP)* line was used to block Bmp signaling via a single heat-shock at A30h. Quantification of the percentage of Hnf4a^{strong} (arrows), Hnf4a^{weak} (arrowheads), and Hnf4a^{absent} (open arrows) cells and of VenusPEST$^+$ cells among H2B-mCherry$^+$ cells. Scale bars: 20 (A–D, F), 150 (E) μm; error bars: ±SEM.
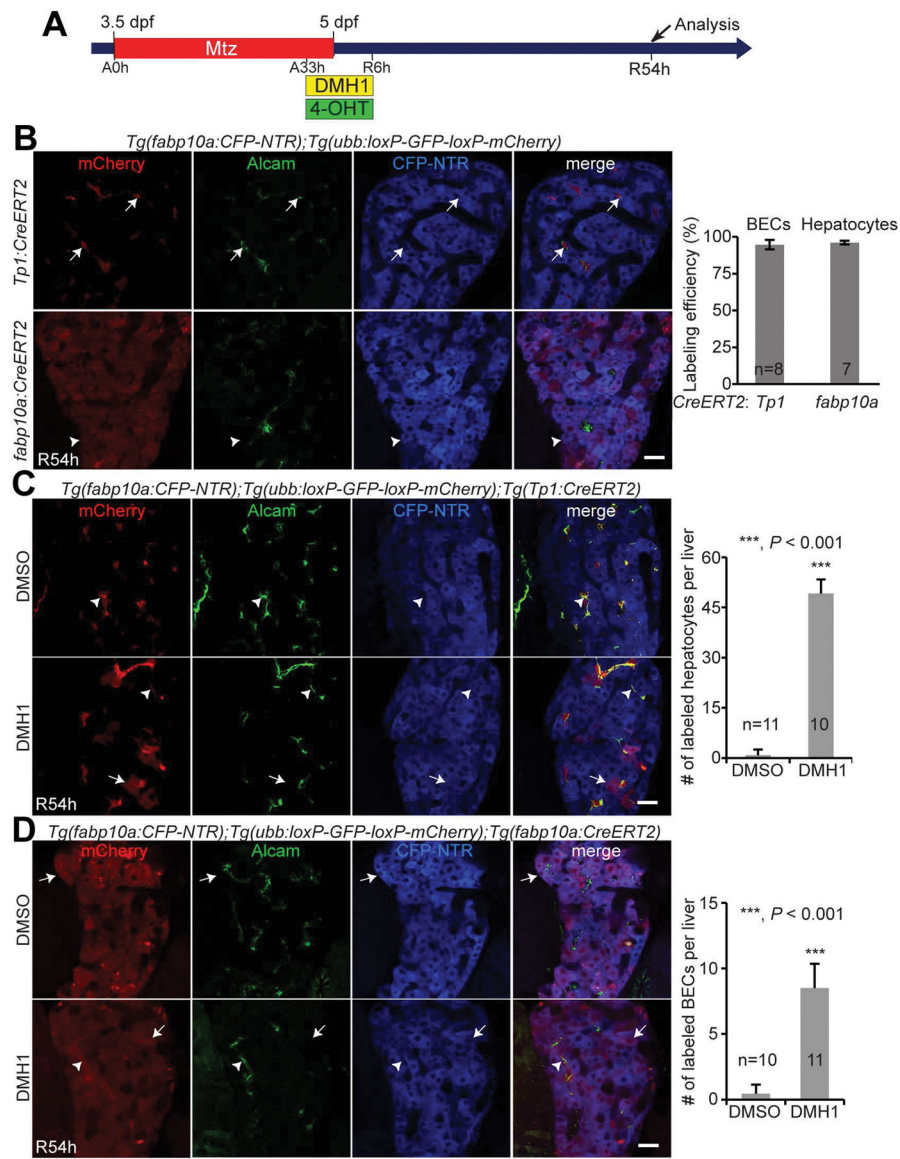
Figure 3. Bmp inhibition maintains HB-LCs as undifferentiated

(A) Experimental scheme illustrating the stages of Mtz, DMH1, and 4-OHT treatment. (B) Labeling efficiency of the lineage tracing with the *Tg(Tp1:CreERT2)* and *Tg(fabp10a:CreERT2)* lines. Arrows point to CFP⁻/mCherry⁺/Alcam⁺ cells (Cre-labeled BECs); arrowheads point to CFP⁺/mCherry⁺/Alcam⁻ cells (Cre-labeled hepatocytes). Quantification of the percentage of the labeled BECs and hepatocytes. (C, D) Single-optical section images showing the expression of mCherry, Alcam, and *fabp10a:*CFP-NTR in regenerating livers at R54h. A Cre reporter line, *Tg(ubb:loxP-GFP-loxP-mCherry)*, was used together with the *Tg(Tp1:CreERT2)* (C) or the *Tg(fabp10a:CreERT2)* (D) line. Arrows point to CFP⁺/mCherry⁺/Alcam⁻ hepatocytes; arrowheads point to CFP⁻/mCherry⁺/Alcam⁺ BECs. Quantification of the numbers of CFP⁺/mCherry⁺/Alcam⁻ hepatocytes and CFP⁻/mCherry⁺/Alcam⁺ BECs per liver. Scale bars: 20 μm; error bars: ±SEM.
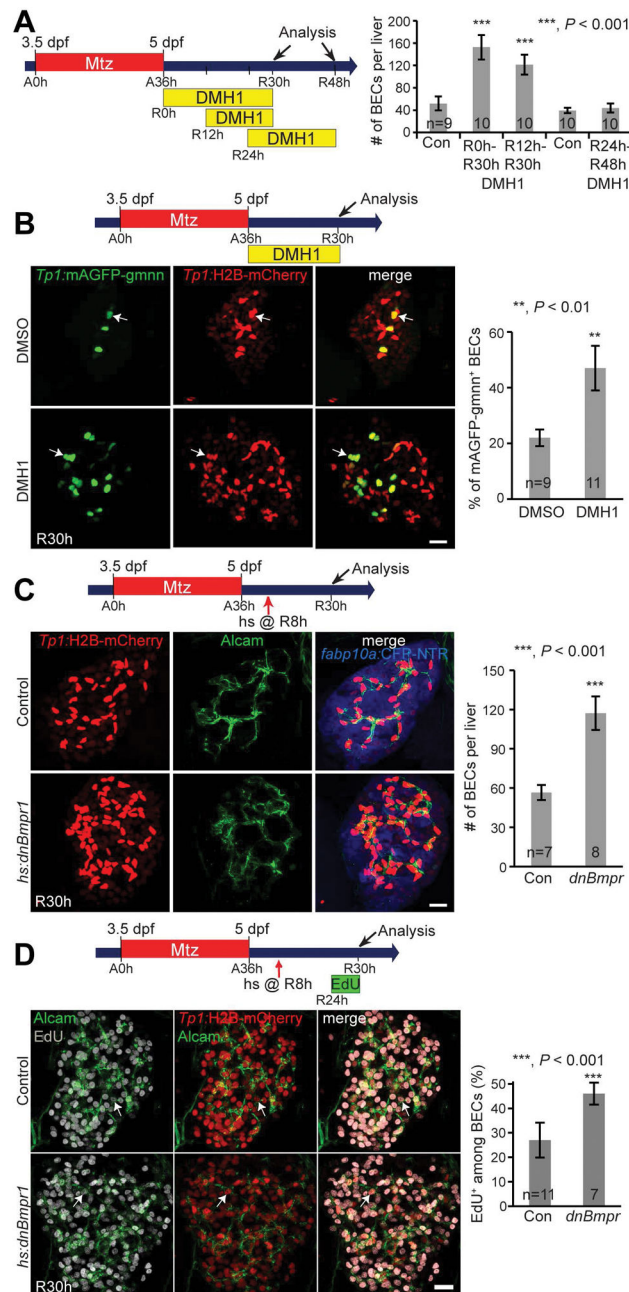
Figure 4. Bmp inhibition after hepatocyte ablation increases BEC number in regenerating livers via proliferation

(A) Experimental scheme illustrating the stages of Mtz and DMH1 treatment. Quantification of the total numbers of BECs in regenerating livers treated with DMH1 for three different time-windows. (B) Confocal projection images showing *Tp1*:H2B-mCherry and *Tp1*:mAGFP-gmnn expression in regenerating livers. Arrows point to mCherry/mAGFP-gmnn double-positive cells. Quantification of the percentage of mAGFP-gmnn^{+} cells among H2B-mCherry[+] BECs. (C) Confocal projection images showing the expression of Alcam, *Tp1*:H2B-mCherry, and *fabp10a*:CFP-NTR in regenerating livers at R30h. Quantification of

the total numbers of BECs (H2B-mCherry$^+$/Alcam$^+$) per liver. (D) Confocal projection images showing EdU labeling and Alcam and *Tp1*:H2B-mCherry expression in regenerating livers. Arrows point to EdU$^+$ BECs. Quantification of the percentage of EdU$^+$ cells among BECs. Scale bars: 20 μm; error bars: ±SEM.
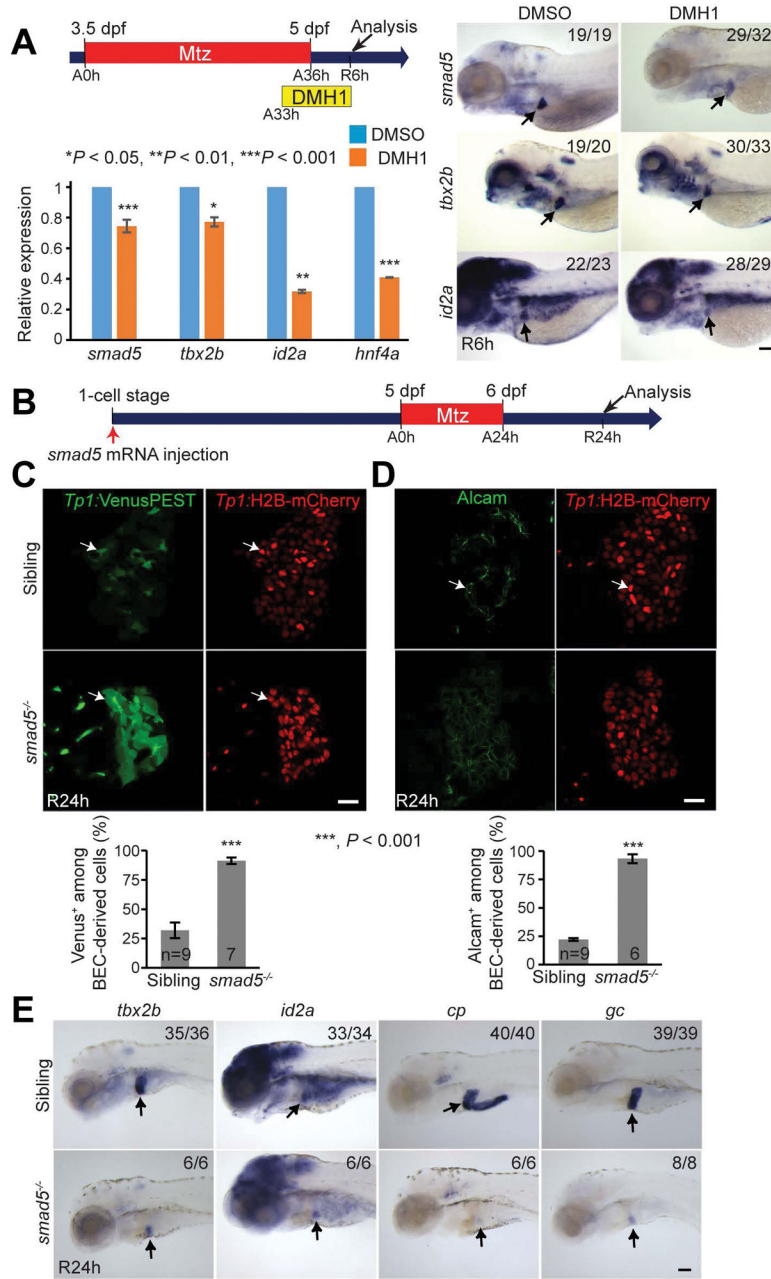
Figure 5. *smad5* mutants exhibit a defect in HB-LC differentiation into hepatocytes
(A) qPCR data showing the relative expression levels of *smad5*, *tbx2b*, *id2a* and *hnf4a* between DMSO- and DMH1-treated regenerating livers at R6h; WISH images showing the expression of *smad5*, *tbx2b* and *id2a* in regenerating livers (arrows). (B) Experimental scheme illustrating the stages of *smad5* mRNA injection (red arrow) and Mtz treatment for C–E. (C) Single-optical section images showing *Tp1:*VenusPEST and *Tp1:*H2B-mCherry expression in regenerating livers. Quantification of the percentage of VenusPEST+ cells among BEC-derived H2B-mCherry+ cells. (D) Single-optical section images showing Alcam and *Tp1:*H2B-mCherry expression in regenerating livers. Quantification of the
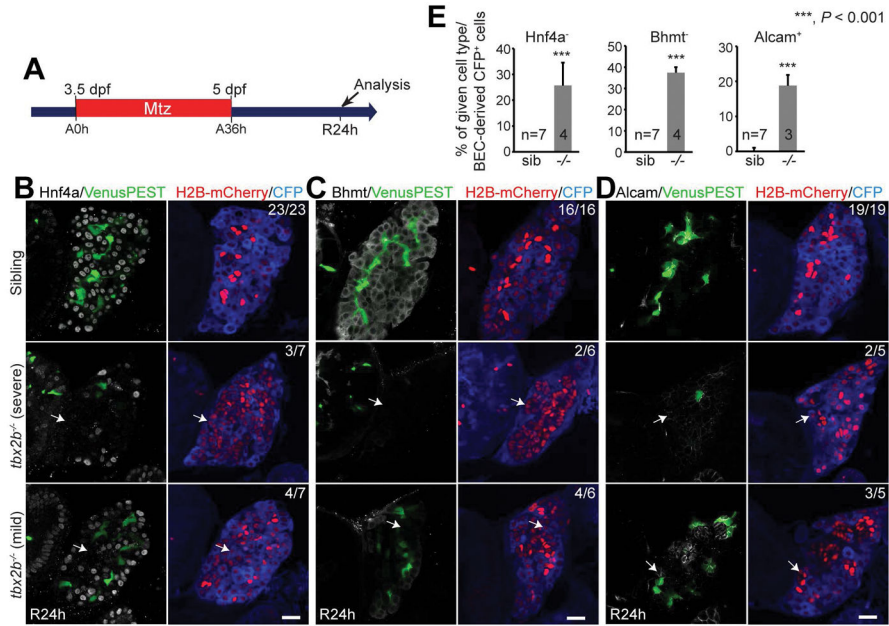
percentage of Alcam$^+$ cells among BEC-derived H2B-mCherry$^+$ cells. (E) WISH images showing the expression of *tbx2b*, *id2a*, *cp* and *gc* in regenerating livers (arrows). Scale bars: 150 (A, E), 20 (C, D) μm; error bars: ±SEM.

Figure 6. *tbx2b* mutants exhibit a defect in HB-LC differentiation into hepatocytes

(A) Experimental scheme illustrating the stage of Mtz treatment and analysis. (B–D) Single-optical section images showing the expression of *fabp10a:*CFP-NTR, *Tp1:*VenusPEST, *Tp1:*H2B-mCherry, and Hnf4a (B), Bhmt (C) or Alcam (D) in regenerating livers. (E) Quantification of the percentage of Hnf4a⁻, Bhmt⁻, or Alcam⁺ cells (arrows) among CFP-NTR⁺/H2B-mCherry⁺ cells as shown in B–D. The mild cases were used for quantification. Scale bars: 20 μm; error bars: ±SEM.
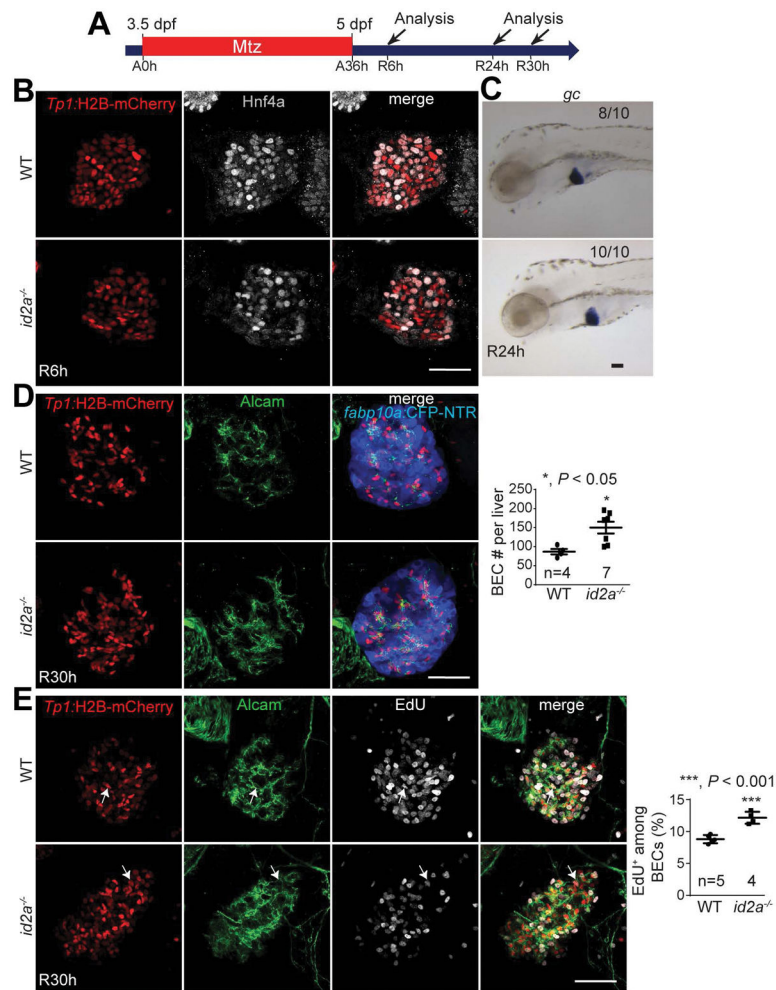
Figure 7. *id2a* mutants have excessive BECs in regenerating livers

(A) Experimental scheme illustrating the stages of Mtz treatment and analysis. (B) Single-optical section images showing Hnf4a and *Tp1*:H2B-mCherry expression in regenerating livers. (C) WISH images showing *gc* expression in regenerating livers. (D) Confocal projection images showing the expression of Alcam, *Tp1*:H2B-mCherry, and *fabp10a*:CFP-NTR in regenerating livers. Quantification of the total numbers of BECs (Alcam[+]/H2B-mCherry[+]) per liver. (E) Confocal projection images showing EdU labeling and Alcam and *Tp1*:H2B-mCherry expression in regenerating livers. EdU was treated from R24h for 6 hours. Arrows point to EdU[+] BECs. Quantification of the percentage of EdU^{+} cells among BECs. Scale bars: 50 μm; error bars: ±SEM.
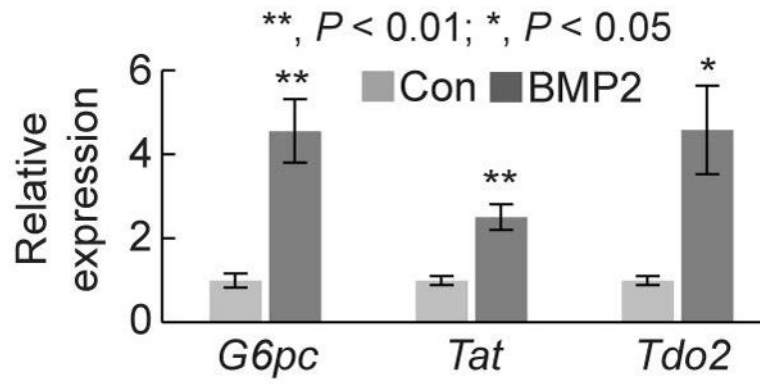
Figure 8. BMP2 treatment promotes the differentiation of a murine LPC cell line into hepatocytes *in vitro*

qPCR data showing the relative expression levels of *G6pc, Tat,* and *Tdo2* between control and BMP2 treatment (n=4). Error bars: ±SEM.